



Research Article

Cellulose hydrolysis catalysed by mesoporous activated carbons functionalized under mild conditions

F.-Z. Azar¹ · M. A. Lillo-Ródenas¹  · M. C. Román-Martínez¹ 

Received: 23 August 2019 / Accepted: 23 November 2019 / Published online: 30 November 2019
© Springer Nature Switzerland AG 2019

Abstract

The catalytic hydrolysis of cellulose allows the transformation of this sustainable and renewable raw material to obtain biofuels and high-added value chemicals. The process requires acidic catalysts, which should be preferably solid in order to make it greener and, thus, this work proposes the use of functionalized carbon materials for such an application. A mesoporous commercial carbon of trade name SA-30, abbreviated as SA in this work, has been chemically treated at room temperature to create acidic surface oxygen functional groups. The prepared carbon catalysts have been thoroughly characterized by N₂ adsorption-desorption at – 196 °C, temperature programmed desorption and X-ray photoelectron spectroscopy. SAS carbon (prepared by treatment with a saturated solution of (NH₄)₂S₂O₈ in 1 M H₂SO₄ and named by adding S to the name of the original carbon) is the most effective of the studied catalysts. It allows achieving high cellulose conversion (about 61%) and glucose selectivity. Thus, the low-cost functionalized carbons prepared at mild conditions are effective and promising catalysts for the transformation of cellulose into glucose.

Keywords Cellulose hydrolysis · Glucose · Carbon materials · Room temperature functionalization

1 Introduction

The conversion of biomass into fuels and chemicals implies the exploitation of a renewable feedstock and can contribute to reduce the world's dependence on fossil fuels. There are many studies devoted to promote the use of biomass with the purpose of achieving a suitable way to replace fossil fuels, contributing, as well, to mitigate the environmental damage caused by their use. An example of these studies can be found in references [1–5]. Nowadays requirements imply that the biomass selected for such a use must be non-edible and agricultural land should not be dedicated to biomass growing, to avoid interference with food production. Thus, mainly lignocellulosic biomass by-products

from agricultural and industrial processes shall be used. Lignocellulosic biomass is constituted by the following three polymeric components: cellulose (C6 units (glucose) with 1-4 β-glycosidic bonds), hemicellulose (mainly C5 units (xylose)) and lignin (amorphous polymer with three phenyl propanolic monomers bound by C–C and ether bonds) [5]. Cellulose, the most abundant component of lignocellulosic biomass, is considered a particularly attractive resource to obtain fuels and useful chemical products [6] and it is also frequently used as a model of lignocellulosic materials. Among the different processes for cellulose conversion into fine chemicals, pyrolysis, microwave cracking, fermentation and hydrolysis, the last one has shown to be very suitable to obtain important feedstock molecules like glucose or

Electronic supplementary material The online version of this article (<https://doi.org/10.1007/s42452-019-1776-6>) contains supplementary material, which is available to authorized users.

✉ M. C. Román-Martínez, mcroman@ua.es | ¹MCMA Group, Department of Inorganic Chemistry and Materials Institute, Faculty of Sciences, University of Alicante, Ap. 99, 03080 Alicante, Spain.



SN Applied Sciences (2019) 1:1739 | <https://doi.org/10.1007/s42452-019-1776-6>

hydroxymethylfurfural [7–9]. Glucose can be considered as the first molecule obtained from cellulose hydrolysis, and it is an important product that can be converted into a broad variety of high-added value chemicals (Scheme 1).

Compared with other methods, hydrolysis is, in general, less costly and more selective. However, as a consequence of the robust structure of cellulose due to the profusion of inter and intra-molecular hydrogen bonds, such a process constitutes a technical and scientific challenge. Cellulose hydrolysis is usually carried out by means of homogeneous catalysis, either by enzymatic reactions [10] or by acidic hydrolysis using mineral acids [7]. However, these techniques present important drawbacks like long reaction time, low catalyst recycling factor, corrosion, etc., and because of that, heterogeneous catalysis using solid acids (e.g., resins, metal oxides, zeolites) has become an interesting, and much “greener”, alternative [11, 12].

Carbon materials have attracted a lot of attention in the field of heterogeneous catalysis. This is due to interesting and tuneable properties like morphology, porosity and surface chemistry, in addition to chemical stability in many liquid media and thermal stability in non-oxidising atmospheres. In fact, they have been frequently used as catalysts and catalysts supports [13]. The presence of Oxygen Functional Groups (OFG) on the carbon surface, particularly in the case of mesoporous carbons, seems to be beneficial for the adsorption of β -1,4 glucan chains, what can help to the cellulose network disintegration. The formation of hydrogen bonds with the glucan chains promotes the hydrolysis of the glycosidic bonds [14]. Examples of this use of carbon materials include the work of Shrotri et al. [15], who modified the carbon surface by air oxidation, but also added diluted HCl to the reaction media to increase the catalyst’s activity, and the works of Hara et al., that

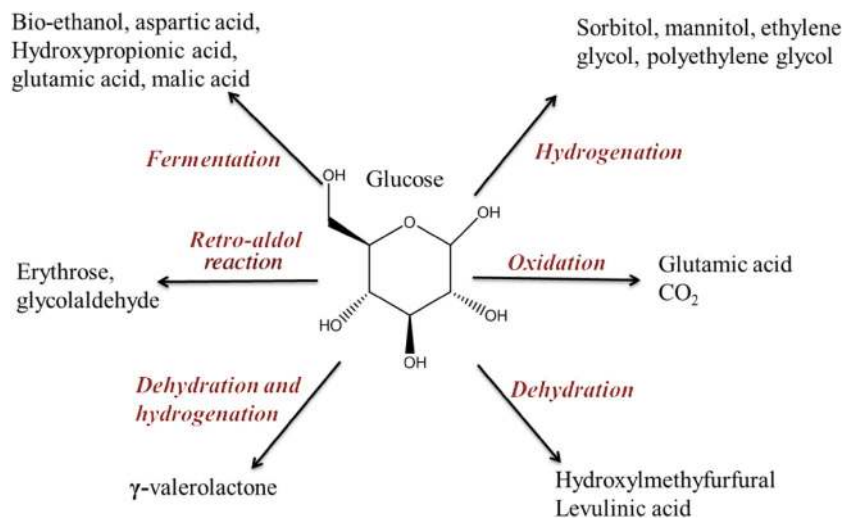
used concentrated H_2SO_4 solution at high temperature to create not only OFG, but also sulfonic groups [14, 16, 17].

The present work is focused on the preparation of carbon based catalysts for the hydrolysis of cellulose, using a commercial mesoporous activated carbon, with the purpose of developing an adequate surface chemistry by oxidation and sulfonation treatments carried out in liquid phase at room temperature. The main objective is to create the suitable amount and type of surface functionalities, especially acidic ones, while retaining the optimum desired textural properties.

The used oxidation method consists of a treatment with a saturated aqueous solution of $(NH_4)_2S_2O_8$ in 1 M H_2SO_4 at room temperature. It has been selected because, as indicated by Moreno-Castilla et al. [18, 19], it introduces strong acidic groups and, furthermore, it does not significantly modify the textural properties of the original activated carbon and, as indicated by Li et al [20], it is non-hazardous, non potentially explosive, economical and highly soluble in water. On the other hand, as sulphuric acid is frequently used to develop sulfonic groups on the carbon surface [17, 21, 22], the carbon resulting after treatment with 1 M H_2SO_4 solution at room temperature (the one used in the ammonium persulfate treatment) has been also considered a potential catalyst. It should be pointed out that these conditions are clearly milder than those usually reported for such a way to create sulfonic groups (for example, concentrated H_2SO_4 at 373 K [22] and 10 M H_2SO_4 at 373 K [21]).

The adopted surface modification strategies involve mild conditions and, thus, they can be regarded as low-cost methods. Detailed analysis of the surface chemistry has been performed to determine the specific surface functionalities that enhance cellulose hydrolysis and selectivity to glucose.

Scheme 1 High added-value chemicals from glucose



Thus, in summary, this work focuses on the development of effective heterogeneous hydrolysis catalysts consisting on functionalized carbon materials, as they have properties scarcely exploited yet for this reaction (like a suitable porosity and a tuneable surface chemistry). The development of such catalysts is desired for the replacement of the commonly used liquid strong acids. This, together with the use of mild conditions for the catalysts preparation (with economic and environmental benefits), and the detailed characterization of the carbon-based catalysts, are the main scientific contributions of this work.

2 Experimental

2.1 Materials

The commercial activated carbon from MeadWestvaco (USA) named SA-30, which is produced by activation using H_3PO_4 , has been selected to prepare the carbon catalyst because of its high surface area and mesopore volume [23]. The carbon, named SA in this work, was treated with the following chemical agents:

1. Saturated solution of $(NH_4)_2S_2O_8$ in aqueous 1 M H_2SO_4 (sample SAS)
2. 1 M H_2SO_4 aqueous solution (sample SASu).

In both cases, the mixture carbon/solution (1 g activated carbon/ 10 ml solution) was maintained under stirring for 24 h at room temperature. Afterwards, the treated carbons were filtered, and then washed several times with distilled water until the filtrate became neutral and sulfates were removed out (determined by $BaCl_2$ testing).

The performance of the carbon catalysts was compared with that of the Amberlyst 15 resin (Sigma Aldrich), a known acidic solid [24, 25].

The commercial microcrystalline Avicel cellulose (99% purity, Sigma Aldrich) was pre-treated by ball-milling in a planetary mill, with agate balls/cellulose weight ratio of 3, at 500 rpm for 7 h with reverse rotation every 60 min [26].

2.2 Characterization

The textural properties of SA, SAS and SASu carbon materials were determined by N_2 adsorption-desorption at $-196^\circ C$ using a Quantachrome Autosorb-6B equipment. The apparent BET surface area (S_{BET}) and the total micropore volume (V_{micro} , volume of pores with diameter lower than 2 nm) were calculated using the BET and Dubinin-Radushkevich equations [27, 28], respectively. The mesopore volume (V_{meso} , volume of pores with diameter between 2 and 20 nm) was estimated as the difference between the

amount of N_2 adsorbed at $P/P_0=0.99$ and at $P/P_0=0.2$ and the total pore volume (V_{tot}) was obtained from the volume of N_2 adsorbed at $P/P_0=0.95$ [29, 30]. The mean pore size was determined by the equation $D=4 \times V_{tot}/S_{BET}$ [28].

The surface chemistry of the carbon catalysts was analysed by temperature programmed desorption (TPD) ($20^\circ C/min$ up to $900^\circ C$, 100 ml/min He flow) using a thermobalance (TA-SDT Q600) coupled to a mass spectrometer (Thermostar, Balzers). This enables the simultaneous record of weight loss, and CO_2 and CO evolution. The surface chemistry of the carbon materials was also characterized by X-ray Photoelectron Spectroscopy (XPS, VG Microtech Multilab ESCA-3000 spectrometer). XPS spectra were obtained using a K-Alpha spectrometer (Thermo-Scientific), with a high resolution monochromator and the following specifications: Al anode (1486.6 eV) X-ray source, 5×10^{-9} mbar analysis chamber pressure and detection in constant energy mode with pass energy of 200 eV for the survey spectrum, and of 50 eV for the sweep in each individual region. Data analysis was performed with the Origin peak fitting software.

Moreover, the amount of acidic sites was determined using a simplified Boehm titration method in which 0.1 g carbon were mixed with 20 ml of a 0.05 M NaOH solution. Then, the mixture was treated in ultrasound bath for 1 h and, after filtration, the solution was titrated with HCl 0.05 M.

The carbon catalysts have been also analysed by TEM in order to characterize their microstructure. JEM-2010 transmission electron microscope from JEOL with an acceleration voltage of 200 kV has been used for this purpose.

The crystallinity of the Avicel cellulose, before and after the milling treatment, was analysed by X-ray diffraction (XRD) using the Miniflex II Rigaku equipment (30 kV/15 mA) with Cu $K\alpha$ radiation and a scanning rate of $2^\circ/min$, in the $6-80^\circ 2\theta$ range. The crystallinity index has been calculated as $CrI (\%) = [(I_{200} - I_{am})/I_{200}] * 100$, where I_{200} and I_{am} are the intensity of the peaks at 22.30° and 18° , respectively [31].

2.3 Catalytic tests

The catalytic tests were performed in a 50 ml stainless steel Parr reactor (Model 4792), lined with a Teflon container. The reaction conditions were chosen after a literature revision and are the following: 500 mg cellulose, 125 mg catalyst, 25 ml distilled water, $190^\circ C$ and 3 h, under stirring. At the end of the experiment, the solid and liquid phases were separated by filtration. The liquid phase was analysed by high performance liquid chromatography (HPLC, 1200 infinity Agilent Technologies, column; Hi-Plex Ca (Duo), 300×6.5 mm) and the solid was dried and weighted to calculate the cellulose conversion.

Conversion, product yield and selectivity were calculated according to the following expressions:

$$\text{Conversion} = [1 - (\text{weight of unreacted cellulose} / \text{weight of charged cellulose})] \times 100$$

$$\text{Yield of A} = [\text{moles of A} / \text{moles of charged cellulose}] \times 100$$

$$\text{Selectivity to A} = [\text{yield of A} / \text{conversion}] \times 100$$

3 Results and discussion

3.1 Cellulose pretreatment

Ball milling is an efficient physical pre-treatment to decrease the cellulose crystallinity, thus facilitating its hydrolysis [32]. Figure 1 shows the XRD results obtained for the original and milled Avicel cellulose, which reveal the important crystallinity decrease produced after the ball-milling treatment.

The calculated crystallinity index (Crl) of the untreated cellulose (Fig. 1a) is 61%, while the XRD profile of the ball-milled cellulose (Fig. 1b) does not allow determining the Crl because, as the material becomes quite amorphous, a clear I_{200} peak can not be distinguished. Therefore, it is evident that the ball-milling pretreatment greatly reduces the crystallinity of this microcrystalline cellulose.

3.2 Catalysts textural properties

Figure 2 shows the N_2 adsorption-desorption isotherms at -196°C obtained for the three carbon materials used as catalysts. They are type IV isotherms according to the IUPAC classification [30], characteristic of mesoporous adsorbents. The relatively high adsorption at low relative pressure indicates that the samples have a significant micropore volume, and the steep slope indicates that their pore size distribution is wide. The pore size distribution graphs are presented as Supplementary

Material (Figure S1) and they show that SA and SASu samples have similar pore size distribution, while SAS

sample has also a wide pore size distribution, but with lower narrow micropore volume. The textural parameters, calculated from the N_2 adsorption-desorption isotherms as indicated in the experimental section, are presented in Table 1.

The SA activated carbon presents high specific surface area and a well-developed porosity, both in the micro and mesopore ranges. The treatment with 1 M H_2SO_4 solution (sample SASu) produces only a slight modification of the porous structure. In contrast, the treatment of SA with the solution of $(NH_4)_2S_2O_8$ in 1 M H_2SO_4 (sample SAS) leads to a significant decrease of the adsorption capacity, which can be due either to destruction of pores, or to porosity blockage by the developed surface oxygen groups, as reported for other carbon materials submitted to a similar treatment [33].

In any case, the three carbon materials used in this work present well-developed mesoporosity and high surface area. As previously reported [34], mesoporosity is useful for the adsorption of β -1,4 glucan chains, which could then be broken on the carbon surface. The Amberlyst 15 resin has low surface area and total pore volume (about $40\text{ m}^2\text{ g}^{-1}$ and $0.2\text{ cm}^3\text{ g}^{-1}$, respectively) [24, 25], much lower than those of the carbon materials.

The micro/nanostructure of the carbon materials, as revealed by TEM, can be observed in Figure S2 (Supplementary Material). It can be seen that it is the expected one for an activated carbon in which the small carbon

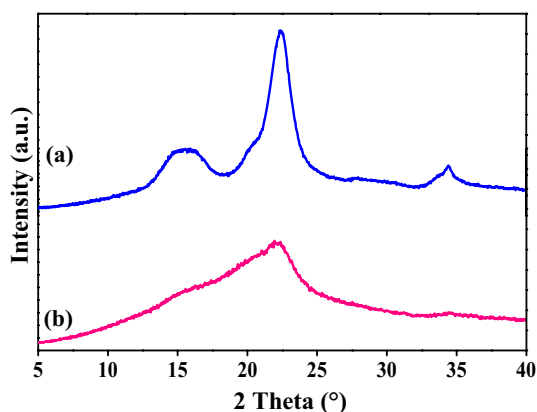


Fig. 1 XRD profiles of Avicel cellulose: (a) untreated, (b) ball-milled

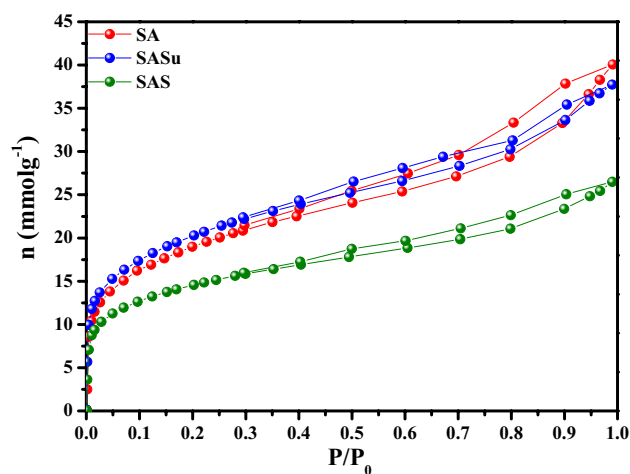


Fig. 2 N_2 adsorption-desorption isotherms at -196°C

Table 1 Textural properties

Sample	S_{BET} (m^2g^{-1})	V_{micro} (cm^3g^{-1})	V_{meso} (cm^3g^{-1})	V_{total} (cm^3g^{-1})	Mean pore size (nm)
SA	1464	0.74	0.73	1.40	3.83
SASu	1522	0.78	0.60	1.24	3.44
SAS	1274	0.56	0.48	0.99	3.11

S_{BET} BET surface area, V_{micro} micropore volume, V_{meso} mesopore volume, V_{total} total pore volume (for details see the text)

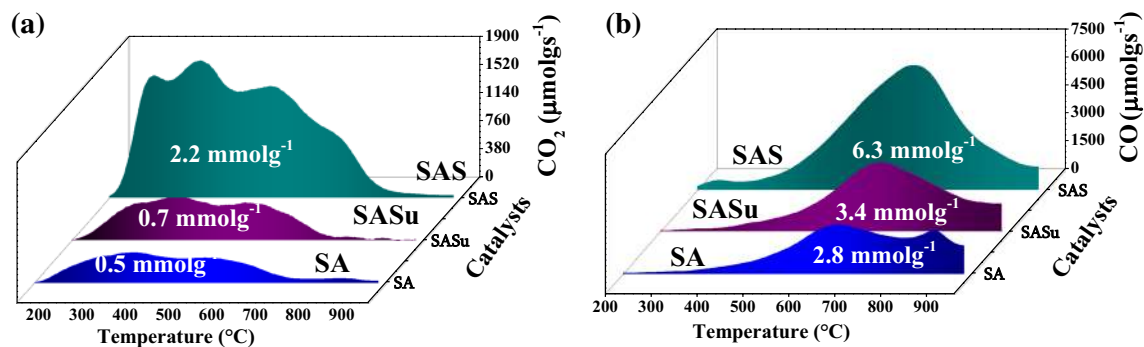


Fig. 3 TPD spectra of SA, SASu and SAS samples: **a** CO_2 evolution and **b** CO evolution

platelets can be observed forming a microcrystalline structure. It must be mentioned that such a structure is not significantly modified by the chemical treatments performed.

3.3 Catalysts surface chemistry

Figure 3 shows the CO_2 and CO evolution profiles obtained in the TPD experiments carried out with the three studied carbon materials. It can be observed that the treatment with 1 M H_2SO_4 leads to the creation of a moderated amount of oxygen functional groups (OFG) on the carbon surface (sample SASu) while, as expected, the oxidation treatment carried out to produce the SAS sample results in much higher development of surface OFG (be aware of the different scale of Fig. 3a and b). The total amount of CO_2 and CO evolved in the TPD measurements, calculated as $\text{CO} + \text{CO}_2$, accounts 3.3, 4.1 and 8.5 mmol g^{-1} for carbons SA, SASu and SAS, respectively. The TG data associated to the TPD experiments (Figure S3, Supplementary Material) show that the mass loss is in agreement with the thermal removal of OFG (comparison of mass loss below 100 °C indicates that SASu sample contained more humidity).

In order to perform a deeper characterization of the surface chemistry, the CO_2 and CO evolution profiles shown in Fig. 3 were deconvoluted with the purpose of determining the amount of different types of OFG (deconvolution is shown in Figure S4 of the Supplementary Material (SM)). For this purpose, deconvolution was done using a multiple Gaussian function and each peak was centred

at temperature values selected according to the literature [20, 35, 36]. The CO_2 evolution peaks corresponding to the decomposition of strongly (SC) and weakly (WC) acidic carboxylic groups are centred in the 230–270 °C and 360–380 °C intervals, respectively. Thus, SC and WC are carboxylic groups that differ in their thermal stability and in the pH that they confer to an aqueous suspension [37]. The TPD peaks due to the decomposition of other functional groups are centred in the following temperature intervals: ~520 to 550 °C—carboxylic anhydride groups (CA); ~650 to 670 °C—lactone groups (LN) at, ~650 to 700 °C—phenol type groups (PH) and 750–943 °C—carbonyl and quinone groups (CQ). These temperature intervals reveal that some OFG can decompose showing overlapped CO_2 and CO desorption peaks.

It should be noted that two low temperature CO peaks (labelled as CO#1 and CO#2) appear in the fitting of the CO evolution profiles. They are centred at temperatures similar to those at which the peaks corresponding to the decomposition of SC and WC carboxylic groups are located. This phenomenon is also reported in literature. Figueiredo and co-workers attributed these peaks to the reaction between CO_2 and the carbon surface [38], while Moreno-Castilla et al. consider that the low temperature CO probably comes from carbonyl groups that come from the decomposition of α -substituted ketones and aldehydes [18].

In the case of SA carbon, CO_2 and CO desorption at ~870 °C (see Fig. 3 and Figure S4) has been explained as a consequence of surface reactions of trace phosphoric

groups remaining from the activation treatment with H_3PO_4 [39, 40]. The absence of such features in the TPD spectra of SASu and SAS samples would indicate that phosphoric groups were mostly eliminated by the treatments with acidic solutions carried out to obtain them from the original SA carbon.

The amount of each type of OFG determined from the areas of the deconvoluted TPD profiles (excluding those related to phosphoric acid in carbon SA) is presented in Table 2. It can be observed that in the original activated carbon, the most abundant OFG are phenol-type groups, followed by carbonyl and quinone groups. The treatment with 1 M H_2SO_4 solution leads to the development of all OFG types, being the increase of strongly acidic carboxylic groups the most pronounced. The treatment with the saturated solution of $(NH_4)_2S_2O_8$ in 1 M H_2SO_4 produces a noticeable increase in the total amount of OFG, which corresponds to the creation of all types of groups. It can be underlined that, compared to SASu, SAS carbon contains less carbonyl-quinone groups (Table 2).

The three samples contain a large amount of acidic OFG (calculated as the sum of SC, WC, CA, PH and LN) and the order regarding the OFG content is $SA < SASu << SAS$.

The acidity of the carbon materials determined by titration (expressed as mmol of acidic sites per gram of carbon, Table 2) follows the same trend, although the differences between samples are less pronounced.

The amount of acidic OFG determined by deconvolution of the TPD spectra has been plotted versus the amount of acidic sites determined by titration, and a linear correlation has been found (Fig. S5, Supplementary Material). However, the difference between the total amount of acidic oxygen groups determined from TPD data and the acidity determined by titration is relatively large. This point could be explained considering that not all the surface functional groups have the same acidity. Thus, titration is the result of an average measurement of groups with different acidity and basicity.

It can be pointed out that the acidity of carbon SAS (4.08 mmol g^{-1} determined by titration) is comparable to the acidity of Amberlyst 15 resin (4.7 mmol g^{-1}) [24]. This strong acidity is expected to enhance the catalytic activity in the hydrolysis of cellulose [14, 41].

The surface chemistry of the carbon materials has been also characterized by means of XPS. Figure 4 shows the O1s XPS spectra of the three studied samples.

Deconvolution of the O1s spectra (Fig. 4) based on the binding energy (B.E.) assignments found in the literature [25, 42, 43] shows peaks centred at the following B.E. values (in eV): (1) 530.7 ± 0.2 , assigned to C=O bond in quinone groups, (2) 531.8 ± 0.2 , related to oxygen in O=C or -OH structures of carbonyl or anhydrides and hydroxyl groups, (3) 533.3 ± 0.2 , attributed to phenol type groups

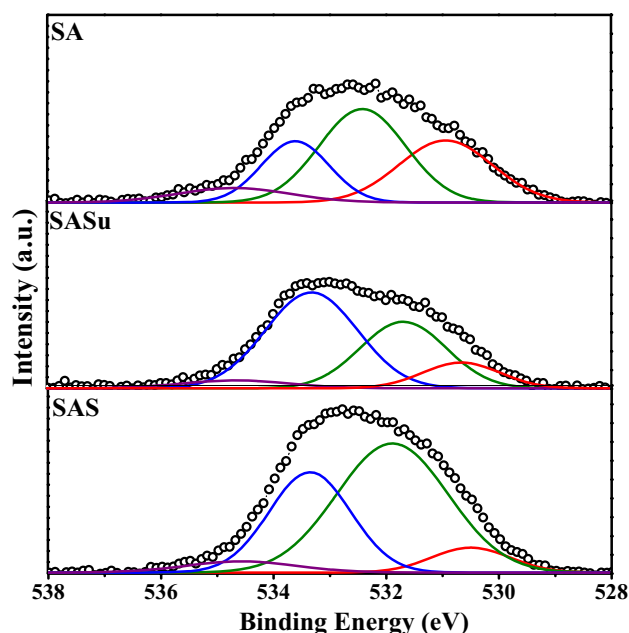


Fig. 4 O 1s XPS data of SA, SASu and SAS

Table 2 Distribution of OFG determined by deconvolution of the TPD profiles and amount of acidic sites measured by titration

Sample	OFG (mmol g^{-1})						Total OFG ^[a] (mmol g^{-1})	Acidic OFG ^[b] (mmol g^{-1})	Acidic sites ^[c] (mmol g^{-1})
	SC	WC	CA	PH	LN	CQ			
SA	0.06	0.18	0.18	1.02	0.04	0.85	2.33	1.48	3.33
SASu	0.11	0.25	0.25	1.50	0.06	1.33	3.50	2.17	3.44
SAS	0.27	0.82	0.93	3.40	0.22	1.16	6.80	5.64	4.08

^aSum of all identified OFG

^bSum of SC, WC, CA, PH and LN groups

^cMeasured by titration

Table 3 O1s XPS data: B.E. (eV), species identification and quantification (at%)

Element	O 1s (at. %)				Acidic OFG [a]
	1	2	3	4	
B.E. (eV)	530.7	531.7	533.3	534.6	Acidic OFG [a]
Formula	C=O	O=C or -OH	C-OH	C=OOH	
Sample					
SA	2.6	3.6	1.9	0.7	6.2
SASu	2.9	4.5	0.4	1.0	5.9
SAS	1.0	7.5	4.3	0.6	12.5

^aSum of acidic OFG (species 2, 3 and 4)

and (4) 534.6 ± 0.2 , assigned to carboxylic groups. Table 3 shows the quantification of the O1s spectra in atomic O percentage (at%) in any of the mentioned oxygen containing surface functionalities.

The contribution of acidic OFG has been calculated assuming that species 2 to 4 (see Table 3) are related with anhydrides and hydroxyl, phenol, and carboxylic acid groups. It can be observed that both, the total amount of oxygen groups and the amount of acidic OFG determined this way, is similar for SA and SASu samples, and clearly higher for SAS.

The C 1s spectra (presented in Figure S6, Supplementary Material) show, apart from the peak centred at about 284.5 ± 0.1 eV due to graphitic C=C, other less intense peaks appearing at 286.0 ± 0.1 eV, 286.7 ± 0.1 eV and 287.5 ± 0.3 eV, which can be attributed to C-O in ether or phenol groups, to quinone or carbonyl groups (C=O), and to carboxylic or carboxylic anhydride groups, respectively. Quantification of the C1s spectra has not been included, as it will be not precise enough because the intensity of the C1s signals due to OFG is low compared to the main peak due to C=C bonds (see Figure S6).

The S 2p XPS spectra of samples SASu and SAS, although with a lot of noise, show a peak located at about 168.1 eV attributed to S in $-\text{SO}_3\text{H}$ groups [44]. This means that sulphur is present in these two samples, although the amount of this element is very low. In fact, the determination of sulphur by elemental analysis shows that the weight concentration of this element in both samples is about 0.1%. Figure S7 in Supplementary Material shows the S 2p XPS spectra of the SAS catalyst before and after the reaction. The profiles obtained are similar, which indicates that the $-\text{SO}_3\text{H}$ groups have not been leached during reaction.

As in the case of the TPD analysis, acidic OFG evaluated by XPS are predominant in all samples (more than 75% of oxygen atoms are present in acidic groups). This is an interesting property of these carbon materials as the interaction between cellulose β -1,4-glucan chains and

acidic OFG on the carbon surface is supposed to favour the breakage of the cellulose network, leading to higher catalytic activity [14].

3.4 Catalytic performance

The hydrolysis of cellulose with the four tested catalysts has led, mainly, to the formation of glucose and hydroxymethylfurfural (HMF). As reported in the literature, the reaction starts with a proton from the acid catalyst interacting with the glycosidic oxygen atoms that link two sugar units, forming a conjugated acid. After addition of water, free sugar and a proton are liberated, and further rehydration and hydrolysis of glucose yields HMF [7, 45].

The obtained values of cellulose conversion and product selectivity are shown in Fig. 5.

Using the original SA carbon, cellulose conversion significantly increases compared to the blank test (56% vs. 35% conversion), leading as well to a higher selectivity to glucose. This means that this activated carbon is a good catalyst for cellulose hydrolysis. After surface functionalization (samples SASu and SAS), the carbon catalysts

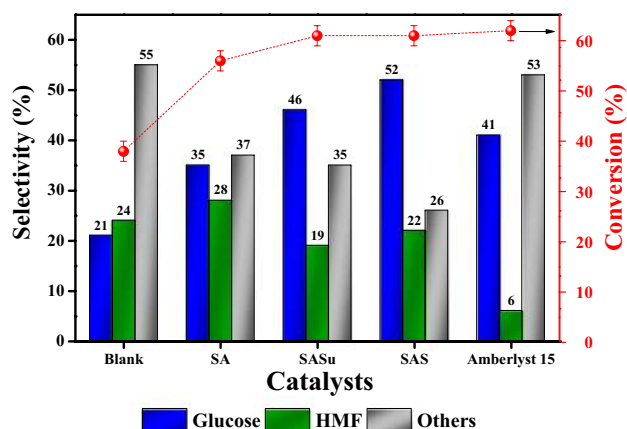


Fig. 5 Cellulose conversion (red points) and products selectivity (HMF: Hydroxymethylfurfural) (500 mg cellulose, 125 mg catalyst, 25 ml distilled water, 190 °C and 3 h)

improve their catalytic performance, leading to 60% cellulose conversion and glucose selectivity close to 50%. In contrast, the commercial Amberlyst 15 resin exhibits a good cellulose conversion (62%), but a lower selectivity to glucose (41%). Besides, as in the case of the blank experiment, the Amberlyst 15 resin renders a high proportion of other products, each of them in low concentration, that have not been completely identified (furfural, ethylene glycol, polyethylenglycol and levulinic acid can be some of these products), meaning that using this catalyst, the main hydrolysis products (glucose and HMF) are highly degraded.

Regarding the effectiveness of the studied catalysts in terms of glucose yield, the obtained results with the carbon catalysts are 17%, 28% and 32% for SA, SASu and SAS, respectively, while 25% is obtained with Amberlyst 15. The glucose yield of the oxidized carbon materials is higher than that of Amberlyst 15 because they afford a similar cellulose conversion and are clearly more selective to glucose. Thus, the oxidized carbon materials are more effective catalysts than the commercial resin Amberlyst 15. On the other hand, they are more active than the SA original carbon, in spite of having lower pore volume and, in the case of SAS, also lower surface area, what can be attributed to the increase in the amount of acidic surface groups. However, the extensive creation of acidic OFG by the oxidation treatment with the $(\text{NH}_4)_2\text{S}_2\text{O}_8$ solution in 1 M H_2SO_4 (SAS sample) does not lead to a further increase of the cellulose conversion respect to the behaviour of the SASu catalyst, and the increase in glucose selectivity is much lower than the increase in the amount of OFG. The increase in selectivity is more pronounced from SA to SASu than from SASu to SAS. This can be explained either by a limit in the positive effect of acidic OFG, by the lower surface area and pore volume, or by a combination of these two reasons. The good catalytic performance of SASu and SAS carbons for cellulose hydrolysis can be also related with the presence of sulfonic groups (detected by XPS). The stability of those groups was proved by their presence in the SAS catalyst surface before and after reaction (Fig. S4, SM).

The obtained results mean that the oxidized carbon materials show a good catalytic performance. However, to support this idea, it is necessary to compare the obtained data with recent results on the topic reported in the literature. Nevertheless, such a comparison is usually not straightforward because the reaction conditions are different, and sometimes the way to express the catalytic activity is different as well. In any case, some reported data have been collected in Table 4, indicating the differences in the operation conditions. The reported data correspond to the use of carbon materials as catalysts, without acid addition, and water as solvent. Explanations and comments on the information presented in the table are given below.

BA-475, an oxidized (air, 475 °C, 3 h) high surface area ($1100 \text{ m}^2 \text{ g}^{-1}$) commercial activated carbon was used as catalyst in a mix-milling process with microcrystalline cellulose (entry 1 [15]) and, although a high cellulose conversion was obtained (with the advantages of high S/C ratio and low reaction time), the glucose yield is moderate, meaning that many by-products have been formed. Besides, the oxidation treatment led to 54% burn-off, which implies a significant loss of solid. Huang et al. (entry 2 [46]), used a graphene oxide prepared from graphite by the harsh Hummers method, and then submitted to a sulfonation treatment (with 98% sulfuric acid). The results are poor using water as solvent (data shown in the table), but they noticeably improve when the solvent is 1/10 (vol/vol) mixture of water and N-dimethylacetamide. Gan et al. (entry 3 [47]) use a lignin derived solid acid (LDSA) sulfonated in concentrated sulfuric acid with quite low S/C ratio (high amount of catalyst). The results are expressed as yield to total reducing sugars (TRS), and because of that, it is not possible to make a proper comparison of glucose yield. Data of entry 4 [48] correspond to a solid acid catalyst prepared by the co-carbonization of cellulose and PVC (as a way of reusing plastic wastes) and to cellulose pretreated in highly concentrated phosphoric acid. The S/C used was low and instead of glucose yield, yield to TRS is presented. In the work of Li et al. (entry 5 [49]) the carbon catalyst is based on coal tar pitch mesocarbon mesobeads (MCMB) submitted to a sulfonation treatment

Table 4 Summary of reported results for several carbon based catalysts in hydrolysis reaction conditions similar to those used in the present work

Entry	Catalyst name	S/C ^a	T (°C)	T (h)	X _{cellulose} (%)	Y _{glucose} (%)	References
1	AC BA-475	6.5	180	0.3	96	27	[15]
2	GO-SO ₃ H	1	130	8	–	1.4	[46]
3	LDSA	0.25	180	4	–	46-TRS	[47]
4	MPCSA	0.5	150	6	–	58-TRS	[48]
5	R-MCMB-SO ₃ H	0.2	140	4	68	66-TRS	[49]
6	G-TsOH	1	170	12	31	16	[50]
7	SAS	4	190	3	60	32	This work

^aSubstrate/catalyst ratio

in concentrated sulfuric acid. Cellulose was previously chemically treated, the S/C is very low and the activity results are also presented as yield to TRS. Finally, the work of Chen et al. (entry 6 [50]) reports the behaviour of several carbon materials prepared from glucose by hydrothermal synthesis and submitted to different treatments. The one indicated in the table shows the best behaviour in terms of glucose yield among those studied.

The comparison with literature results shows that the carbon catalysts prepared in the present work, particularly SAS, can be considered among the best ones because they lead to a high cellulose conversion and good glucose yield, using water as solvent, a relatively high S/C ratio and short reaction time, although the reaction temperature is somewhat higher. It is important to point out that the SAS carbon leads to the lowest amount of by-products, being 74% the global selectivity to interesting products (glucose and HMF). Besides, the carbon catalysts used in this work have been obtained from a commercial activated carbon and the treatments performed to modify the surface chemistry can be considered mild, in contrast with the more complex and costly treatments reported in most publications.

In summary, the low-cost (mild conditions) modified carbon materials developed in this work combine the required acidity and suitable textural properties, and because of that, they perform better than the Amberlyst 15 resin and some other carbon materials reported in the literature. Amberlyst 15 has low surface area and porosity and a high acidity, which promotes side reactions, converting cellulose or glucose to other by-products. Also, the carbon materials used in this work can be considered advantageous when compared to the resin and other carbon materials because of their lower price or easier (and cheaper) preparative procedures.

4 Conclusions

Low-cost solid acid catalysts for cellulose hydrolysis have been prepared by the modification under mild conditions of the surface chemistry of a commercial mesoporous activated carbon. The three studied carbon catalysts are active for cellulose conversion, and the two oxidized ones show a high selectivity to glucose. Because of that, they show a better performance (higher glucose yield and less by-products) than the commercial Amberlyst 15 resin. SAS carbon (prepared by treatment with a saturated solution of $(\text{NH}_4)_2\text{S}_2\text{O}_8$ in 1 M H_2SO_4) is the most effective of the studied catalysts, leading to 61% cellulose conversion and 52% selectivity to glucose. This good behaviour can be attributed to a proper combination of high OFG amount and suitable porosity. Acidic OFG were found to

play a key role in improving the catalytic performance of carbon materials for cellulose hydrolysis and selectivity to glucose, but the presence of a small amount of sulfonic groups also seems to be relevant.

Acknowledgements The authors thank Ministerio de Ciencia, Innovación y Universidades (RTI2018-095291-B-I00), GV/FEDER (PROMETEOII/2014/010) and University of Alicante (VIGROB-136) for financial support. F.-Z. Azar thanks the AECID (research scholarship for development (2015/2016)) and University of Alicante (cooperation programs for development) for financial support.

Compliance with ethical standards

Conflict of interest On behalf of all authors, the corresponding author states that there is no conflict of interest.

References

1. Serrano-Ruiz JC, Dumesic JA (2011) Catalytic routes for the conversion of biomass into liquid hydrocarbon transportation fuels. *Energy Environ Sci* 4:83–99. <https://doi.org/10.1039/C0EE00436G>
2. Kunkes EL, Simonetti DA, West RM et al (2008) Catalytic conversion of biomass to monofunctional hydrocarbons and targeted liquid-fuel classes. *Science* 322:417–421. <https://doi.org/10.1126/science.1159210>
3. Stöcker M (2008) Biofuels and biomass-to-liquid fuels in the biorefinery: catalytic conversion of lignocellulosic biomass using porous materials. *Angew Chem Int Ed* 47:9200–9211. <https://doi.org/10.1002/anie.200801476>
4. Kamm B, Grüber PR, Kamm M (2015) Biorefineries—industrial processes and products. In: Ullmann's encyclopedia of industrial chemistry. Wiley-VCH Verlag GmbH & Co. KGaA, Weinheim. https://doi.org/10.1002/14356007.i04_j01.pub2
5. Zhou C, Xia X, Lin C et al (2011) Catalytic conversion of lignocellulosic biomass to fine chemicals and fuels. *Chem Soc Rev* 40:5588–5617. <https://doi.org/10.1039/c1cs15124j>
6. Van De Vyver S, Geboers J, Jacobs PA, Sels BF (2011) Recent advances in the catalytic conversion of cellulose. *ChemCatChem* 3:82–94. <https://doi.org/10.1002/cctc.201000302>
7. Fan L, Gharpuray MM, Lee Y-H (1987) Cellulose hydrolysis. Springer, Berlin
8. Liu M, Jia S, Gong Y et al (2013) Effective hydrolysis of cellulose into glucose over sulfonated sugar-derived carbon in an ionic liquid. *Ind Eng Chem Res* 52:8167–8173. <https://doi.org/10.1021/ie400571e>
9. Rinaldi R, Schüth F (2009) Acid hydrolysis of cellulose as the entry point into biorefinery schemes. *ChemSuschem* 2:1096–1107. <https://doi.org/10.1002/cssc.200900188>
10. Zhang YHP, Lynd LR (2004) Toward an aggregated understanding of enzymatic hydrolysis of cellulose: noncomplexed cellulase systems. *Biotechnol Bioeng* 88:797–824. <https://doi.org/10.1002/bit.20282>
11. Rinaldi R, Schüth F (2009) Design of solid catalysts for the conversion of biomass. *Energy Environ Sci* 2:610–626. <https://doi.org/10.1039/b902668a>
12. Aspromonte SG, Romero A, Boix AV, Alonso E (2019) Hydrolysis of cellulose to glucose by supercritical water and silver

- mesoporous zeolite catalysts. *Cellulose* 26:2471–2485. <https://doi.org/10.1007/s10570-018-2221-5>
13. Serp P, Figueiredo JL (2009) Carbon materials for catalysis. Wiley, Hoboken
 14. Kitano M, Yamaguchi D, Suganuma S et al (2009) Adsorption-enhanced hydrolysis of β -1,4-glucan on graphene-based amorphous carbon bearing SO_3H , COOH , and OH groups. *Langmuir* 25:5068–5075. <https://doi.org/10.1021/la8040506>
 15. Shrotri A, Kobayashi H, Fukuoka A (2016) Air oxidation of activated carbon to synthesize a biomimetic catalyst for hydrolysis of cellulose. *Chemsuschem* 9:1299–1303. <https://doi.org/10.1002/cssc.201600279>
 16. Suganuma S, Nakajima K, Kitano M et al (2008) Hydrolysis of cellulose by amorphous carbon bearing SO_3H , COOH , and OH groups. *J Am Chem Soc* 130:12787–12793. <https://doi.org/10.1021/ja803983h>
 17. Nakajima K, Hara M (2012) Amorphous carbon with SO_3H groups as a solid Brønsted acid catalyst. *ACS Catal* 2:1296–1304. <https://doi.org/10.1021/cs300103k>
 18. Moreno-Castilla C, Carrasco-Marín F, Mueden A (1997) The creation of acid carbon surfaces by treatment with $(\text{NH}_4)_2\text{S}_2\text{O}_8$. *Carbon* 35:1619–1626. [https://doi.org/10.1016/S0008-6223\(97\)00121-8](https://doi.org/10.1016/S0008-6223(97)00121-8)
 19. Moreno-Castilla C, Ferro-García MA, Joly JP et al (1995) Activated carbon surface modifications by nitric acid, hydrogen peroxide, and ammonium peroxydisulfate treatments. *Langmuir* 11:4386–4392. <https://doi.org/10.1021/la00011a035>
 20. Li N, Ma X, Zha Q et al (2011) Maximizing the number of oxygen-containing functional groups on activated carbon by using ammonium persulfate and improving the temperature-programmed desorption characterization of carbon surface chemistry. *Carbon* 49:5002–5013. <https://doi.org/10.1016/j.carbon.2011.07.015>
 21. Foo GS, Van Pelt AH, Krötschel D et al (2015) Hydrolysis of cellobiose over selective and stable sulfonated activated carbon catalysts. *ACS Sustain Chem Eng* 3:1934–1942. <https://doi.org/10.1021/acssuschemeng.5b00530>
 22. Fraile JM, García-Bordejé E, Pires E, Roldán L (2014) New insights into the strength and accessibility of acid sites of sulfonated hydrothermal carbon. *Carbon* 77:1157–1167. <https://doi.org/10.1016/j.carbon.2014.06.059>
 23. Marco-Lozar JP, Cazorla-Amorós D, Linares-Solano A (2007) A new strategy for germanium adsorption on activated carbon by complex formation. *Carbon* 45:2519–2528. <https://doi.org/10.1016/j.carbon.2007.08.020>
 24. Kunin R, Meitzner E, Oline J (1962) Characterization of Amberlyst 15. *IEC Prod Res Dev* 1:140–144
 25. Siril PF, Cross HE, Brown DR (2008) New polystyrene sulfonic acid resin catalysts with enhanced acidic and catalytic properties. *J Mol Catal A Chem* 279:63–68. <https://doi.org/10.1016/j.molcata.2007.10.001>
 26. Adsuar-García MD (2017) Catalizadores bifuncionales para la hidrogenación hidrolítica de la celulosa. Ph.D. thesis, University of Alicante
 27. Gregg SJ, Sing KSW (1999) Adsorption, surface area and porosity. Academic Press, New York
 28. Rouquerol F, Rouquerol J, Sing K (1999) Adsorption by powders and porous solids. Principles, methods and applications, 1st edn. Academic Press, San Diego
 29. Rodríguez-Reinoso F, Linares-Solano A (1989) Chemistry and physics of carbon, vol 21. Marcel Dekker Inc, New York
 30. Thommes M, Kaneko K, Neimark AV et al (2015) Physisorption of gases, with special reference to the evaluation of surface area and pore size distribution (IUPAC Technical Report). *Pure Appl Chem* 87:1051–1069
 31. Das K, Ray D, Bandyopadhyay NR, Sengupta S (2010) Study of the properties of microcrystalline cellulose particles from different renewable resources by XRD, FTIR, nanoindentation, TGA and SEM. *J Polym Environ* 18:355–363
 32. Avolio R, Bonadies I, Capitani D et al (2012) A multitechnique approach to assess the effect of ball milling on cellulose. *Carbohydr Polym* 87:265–273. <https://doi.org/10.1016/j.carbpol.2011.07.047>
 33. Rufete-Beneite M, Román-Martínez MC, Linares-Solano A (2014) Insight into the immobilization of ionic liquids on porous carbons. *Carbon* 77:947–957. <https://doi.org/10.1016/j.carbon.2014.06.009>
 34. Chung P-W, Charmot A, Click T et al (2015) Importance of internal porosity for glucan adsorption in mesoporous carbon materials. *Langmuir* 31:7288–7295. <https://doi.org/10.1021/acs.langmuir.5b01115>
 35. Figueiredo JL, Pereira MFR, Freitas MMA, Órfão JJM (1999) Modification of the surface chemistry of activated carbons. *Carbon* 37:1379–1389. [https://doi.org/10.1016/S0008-6223\(98\)00333-9](https://doi.org/10.1016/S0008-6223(98)00333-9)
 36. Domingo-García M, López Garzón FJ, Pérez-Mendoza MJ (2002) On the characterization of chemical surface groups of carbon materials. *J Colloid Interface Sci* 248:116–122. <https://doi.org/10.1006/jcis.2001.8207>
 37. Boehm H (2002) Surface oxides on carbon and their analysis: a critical assessment. *Carbon* 40:145–149. [https://doi.org/10.1016/S0008-6223\(01\)00165-8](https://doi.org/10.1016/S0008-6223(01)00165-8)
 38. Figueiredo JL, Pereira MFR, Freitas MMA, Órfão JJM (2007) Characterization of active sites on carbon catalysts. *Ind Eng Chem Res* 46:4110–4115. <https://doi.org/10.1021/ie061071v>
 39. Li Y, Zhang X, Yang R et al (2015) The role of H_3PO_4 in the preparation of activated carbon from NaOH-treated rice husk residue. *RSC Adv* 5:32626–32636. <https://doi.org/10.1039/C5RA04634C>
 40. Valero-Romero MJ, García-Mateos FJ, Rodríguez-Mirasol J, Cordero T (2017) Role of surface phosphorus complexes on the oxidation of porous carbons. *Fuel Process Technol* 157:116–126. <https://doi.org/10.1016/j.fuproc.2016.11.014>
 41. Huang Y-B, Fu Y (2013) Hydrolysis of cellulose to glucose by solid acid catalysts. *Green Chem* 15:1095–1111. <https://doi.org/10.1039/C3GC40136G>
 42. Oh YJ, Yoo JJ, Il Kim Y et al (2014) Oxygen functional groups and electrochemical capacitive behavior of incompletely reduced graphene oxides as a thin-film electrode of supercapacitor. *Electrochim Acta* 116:118–128. <https://doi.org/10.1016/j.electacta.2013.11.040>
 43. Velo-Gala I, López-Peñalver JJ, Sánchez-Polo M, Rivera-Utrilla J (2014) Surface modifications of activated carbon by gamma irradiation. *Carbon* 67:236–249. <https://doi.org/10.1016/j.carbon.2013.09.087>
 44. Russo PA, Antunes MM, Neves P et al (2014) Solid acids with SO_3H groups and tunable surface properties: versatile catalysts for biomass conversion. *J Mater Chem A* 2:11813–11824. <https://doi.org/10.1039/C4TA02320J>
 45. Xiang Q, Lee EE, Petterson PO, Torget RW (2003) Heterogeneous aspects of acid hydrolysis of α -cellulose. *Appl Biochem Biotechnol* 107:505–514
 46. Huang L, Ye H, Wang S et al (2018) Enhanced hydrolysis of cellulose by highly dispersed sulfonated graphene oxide. *BioResources* 13:8853–8870
 47. Gan L, Zhu J (2018) A ligning derived carbonaceous acid for efficient catalytic hydrolysis of cellulose. *J Bioresour Bioprod* 3:166–171. <https://doi.org/10.21967/jbb.v3i4.9>
 48. Yuan S, Li T, Wang Y et al (2019) Double-adsorption functional carbon based solid acids derived from coprolysis of PVC and PE for cellulose hydrolysis. *Fuel* 237:895–902. <https://doi.org/10.1016/j.fuel.2018.10.088>

49. Li H-X, Zhang X, Wang Q et al (2018) Preparation of the recycled and regenerated mesocarbon microbeads-based solid acid and its catalytic behaviors for hydrolysis of cellulose. *Bioresour Technol* 270:166–171. <https://doi.org/10.1016/j.biortech.2018.09.037>
50. Chen G, Wang X, Jiang Y et al (2019) Insights into deactivation mechanism of sulfonated carbonaceous solid acids probed

by cellulose hydrolysis. *Catal Today* 319:25–30. <https://doi.org/10.1016/j.cattod.2018.03.069>

Publisher's Note Springer Nature remains neutral with regard to jurisdictional claims in published maps and institutional affiliations.